J|A|C|S
ARTICLES
Published on Web 04/05/2006

The Paradoxical Thermodynamic Basis for the Interaction of Ethylene Glycol, Glycine, and Sarcosine Chains with Bovine Carbonic Anhydrase II: An Unexpected Manifestation of Enthalpy/Entropy Compensation

Vijay M. Krishnamurthy, Brooks R. Bohall, Vincent Semetey,† and George M. Whitesides*

Contribution from the Department of Chemistry and Chemical Biology, Harvard University, 12 Oxford Street, Cambridge, Massachusetts 02138

Received January 4, 2006; E-mail: gwhitesides@gmwgroup.harvard.edu

Abstract: This paper describes a systematic study of the thermodynamics of association of bovine carbonic anhydrase II (BCA) and *para*-substituted benzenesulfonamides with chains of oligoglycine, oligosarcosine, and oligoethylene glycol of lengths of one to five residues. For all three of these series of ligands, the enthalpy of binding became less favorable, and the entropy less unfavorable, as the chain length of the ligands increased. The dependence on chain length of the enthalpy was almost perfectly compensated by that of the entropy; this compensation resulted in dissociation constants that were independent of chain length for the three series of ligands. Changes in heat capacity were independent of chain length for the three series and revealed that the amount of molecular surface area buried upon protein−ligand complexation did not increase with increasing chain length. Taken together, these data refute a model in which the chains of the ligands interact hydrophobically with the surface of BCA. To explain the data, a model is proposed based on decreasing "tightness" of the protein−ligand interface as the chain length of the ligand increases. This decreasing tightness, as the chain length increases, is reflected in a less favorable enthalpy (due to fewer van der Waals contacts) and a less unfavorable entropy (due to greater mobility of the chain) of binding for ligands with long chains than for those with short chains. Thus, this study demonstrates a surprising example of enthalpy/entropy compensation in a well-defined system. Understanding this compensation is integral to the rational design of high-affinity ligands for proteins.

Introduction

This paper characterizes the thermodynamics of association of bovine carbonic anhydrase II (BCA, EC 4.2.1.1) with ligands designed to test the interplay between enthalpy and entropy of binding. The ligands used were *para*-substituted benzenesulfonamides (p-$H_2NSO_2C_6H_4CONRR'$) of structure **1**, where

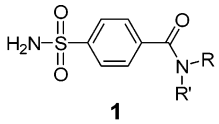

1

$ArEG_nOMe$, R' = H, R = $CH_2CH_2O(CH_2CH_2O)_{n-1}CH_3$

$ArGly_nO^-$, R' = H, R = $CH_2CO(NHCH_2CO)_{n-1}O^-$

$ArSar_nO^-$, R' = CH_3, R = $CH_2CO(N(CH_3)CH_2CO)_{n-1}O^-$

R′ = H or CH_3; the variable parts of these ligands were the R groups, oligoethylene glycol ($ArEG_nOMe$), oligoglycine ($ArGly_nO^-$), or oligosarcosine ($ArSar_nO^-$) chains, where $n = 1-5$. We were interested in these families of ligands for three reasons:

(i) Oligoethylene glycol (EG_n), oligoglycine (Gly_n), and oligosarcosine (Sar_n) chains are commonly used as linkers in the design and synthesis of multivalent ligands.[1−6] Understanding why these flexible linkers can be effective as components in high-avidity ligands (when simple considerations of entropy predict that they would not be)[2,7] will aid in the design of multivalent ligands (Figure 1).

(ii) The system of BCA and p-$H_2NSO_2C_6H_4CONHR$ is the simplest one that we know for studying protein−ligand interactions.[8−10] BCA has been well-defined structurally using biophysical tools (particularly X-ray crystallography).[9,10] It binds most *para*-substituted benzenesulfonamides with the same

† Current address: Laboratoire de Physicochimie, UMR 168, Institut Curie, 26 rue d'Ulm, 75248 Paris, France Cedex 05.

(1) Mammen, M.; Choi, S.-K.; Whitesides, G. M. *Angew. Chem., Int. Ed. Engl.* **1998**, *37*, 2755−2794.
(2) Krishnamurthy, V. M.; Estroff, L. A.; Whitesides, G. M. In *Fragment-based Approaches in Drug Discovery*; Jahnke, W., Erlanson, D. A., Eds.; Wiley-VCH: Weinheim, in press.
(3) Choi, S.-K. *Synthetic Multivalent Molecules: Concepts and Biomedical Applications*; John Wiley & Sons: Hoboken, NY, 2004.
(4) Kiessling, L. L.; Strong, L. E.; Gestwicki, J. E. In *Annu. Rep. Med. Chem.*; Hagmann, W., Doherty, A., Eds.; 2000; Vol. 35, pp 321−330.
(5) Kiessling, L. L.; Gestwicki, J. E.; Strong, L. E. *Curr. Opin. Chem. Biol.* **2000**, *4*, 696−703.
(6) Mulder, A.; Huskens, J.; Reinhoudt, D. N. *Org. Biomol. Chem.* **2004**, *2*, 3409−3424.
(7) Mammen, M.; Shakhnovich, E. I.; Whitesides, G. M. *J. Org. Chem.* **1998**, *63*, 3168−3175.
(8) Colton, I. J.; Carbeck, J. D.; Rao, J.; Whitesides, G. M. *Electrophoresis* **1998**, *19*, 367−382.
(9) Urbach, A. R.; Whitesides, G. M. Manuscript in preparation.
(10) Christianson, D. W.; Fierke, C. A. *Acc. Chem. Res.* **1996**, *29*, 331−339.

10.1021/ja060070r CCC: $33.50

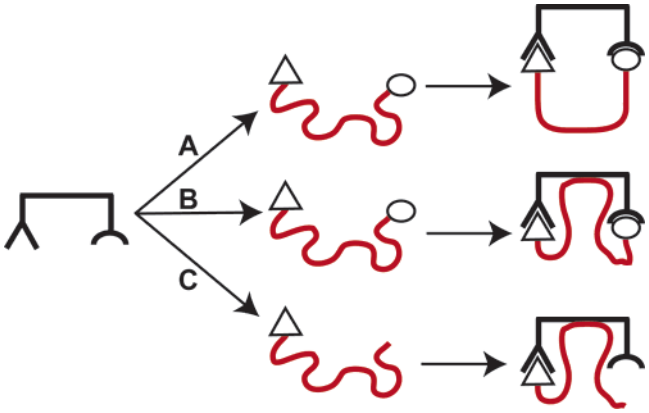

Figure 1. Binding of a bivalent ligand containing a flexible linker (shown in red) to a bivalent receptor. (**A**) We expect the binding process to suffer from an entropic penalty due to the loss in conformational entropy of the linker, which has fewer allowed conformations after complexation than before. (**B**) The linker could interact with the receptor and provide a favorable enthalpy that could partially compensate for the unfavorable conformational entropy. (**C**) The ligand contains only one binding element and the "linker". We study this type of structure in this paper to examine directly the effect of the linker (or chain) on the binding of the ligand to the receptor.

geometry (the ionized sulfonamide nitrogen, $ArSO_2NH^-$, binds to the Zn^{II} cofactor, and the phenyl ring interacts directly with a hydrophobic pocket of the enzyme) (Figure 2); this geometry is independent of the nature of R. This consistent mode of binding allows us to consider the interaction of R (here, the oligomeric chain) with the surface of BCA with high confidence that we know how the phenyl ring (and thus, R) is positioned in the active site. Thus, this system *perturbs* a known interaction, rather than probing an undefined and/or variable one. Perturbation approaches are often the simplest ones to use in working on complicated problems.

(iii) We previously measured the dissociation constants (K_d) for two of the series of ligands ($ArEG_nOMe$ and $ArGly_mO^-$; $n = 1-5$ and $m = 1-6$) and found an entirely unexpected result: these values of K_d were approximately *independent* of chain length for *both* series ($ArEG_nOMe$, $K_d \sim 0.16\ \mu M$ and $ArGly_mO^-$, $K_d \sim 0.33\ \mu M$) and similar to that for unsubstituted benzenesulfonamide ($K_d \sim 0.20\ \mu M$).[11] We had anticipated that values of K_d for sulfonamides with EG_n and Gly_n chains would decrease monotonically with increasing chain length (reflecting an increase in the hydrophobic surface area buried upon protein−ligand complexation) and level off when the number of residues in the chain exceeded the depth of the conical cleft of the enzyme (~15 Å). (This type of behavior characterizes the interaction of CA with *para*-substituted benzenesulfonamides where the R groups are alkyl chains;[11,12] for HCA, K_d decreases from 83 nM for R = methyl to 1.3 nM for R = *n*-hexyl and to 1.2 nM for R = *n*-heptyl.[11]) The insensitivity of K_d to chain length that we observed was particularly difficult to rationalize because the interaction of the chains for $ArGly_mO^-$ with the protein was sufficiently strong to decrease the NMR T_2 relaxation times of the α (or methylene) protons of the first three residues of these chains to <25 ms (the value for these residues when free in solution was 230 ms).[13] The chains were

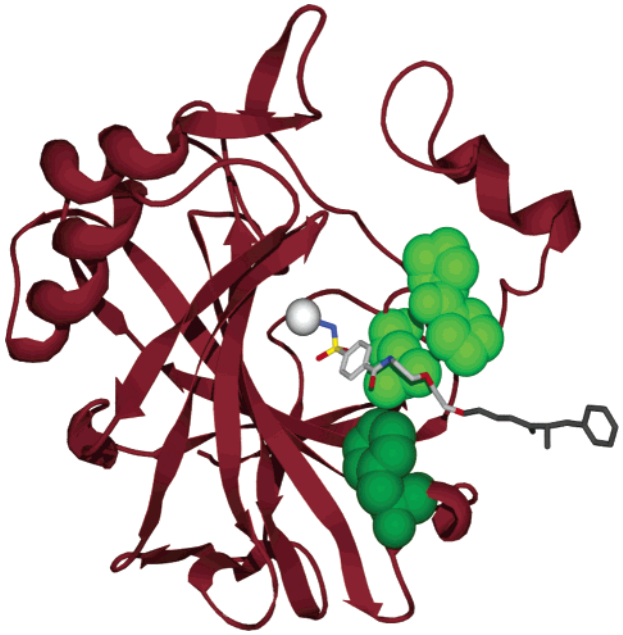

Figure 2. Model for the interaction of $p\text{-}H_2NSO_2C_6H_4CONH(CH_2CH_2O)_2\text{-}CH_2CH_2NHCOPheNH_3^+$ ($ArEG_3PheNH_3^+$) with HCA II based on the deposited X-ray crystallographic coordinates (PDB: 1CNY).[14] HCA has been depicted as a red ribbon diagram with the hydrophobic residues that are within van der Waals contact distance of the ligand rendered as green space-filling models and the catalytically essential Zn^{II} depicted as a gray sphere. The ligand has been rendered as a ball-and-stick model. The light green space-filling residues, Leu-198, Pro-201, and Pro-202, constitute the so-called hydrophobic wall of CA and form the majority of contacts (both hydrophobic and van der Waals) with the oligoethylene glycol linker of the ligand. The dark green residue, Phe-131, has a significant amount of hydrophobic surface buried in the complex with the ligand. The last glycol unit and the Phe residue of the ligand were both disordered and thus not visualized in the crystal structure. They have been modeled using stereochemical constraints and are shown in dark gray. This model was created with POV−Ray (Persistence of Vision Pty. Ltd. (2004). http://www.povray-.org/).

also sufficiently ordered that we were able to locate the first three residues of the chains (of both the $ArGly_mO^-$ and $ArEG_n$-OMe series) in contact with a hydrophobic patch (the so-called "hydrophobic wall") of CA in X-ray structures of the protein−ligand complexes (Figure 2).[14,15] The principal inference from these studies was that the first three residues of the chains for $ArEG_nOMe$ and $ArGly_mO^-$ interacted in a similar fashion (apparently through hydrophobic contacts) with the hydrophobic wall of CA but that, counter to our expectations, this interaction had no effect on the value of K_d.

To explain these results, we proposed a form of enthalpy/entropy compensation[16−21] and hypothesized that longer chains interacted more favorably enthalpically with the surface of BCA (because of greater van der Waals contacts, etc.)[22] than shorter ones but that this interaction was disfavored entropically

(11) King, R. W.; Burgen, A. S. V. *Proc. R. Soc. London B* **1976**, *193*, 107−125.
(12) Gao, J.; Qiao, S.; Whitesides, G. M. *J. Med. Chem.* **1995**, *38*, 2292−2301.
(13) Jain, A.; Huang, S. G.; Whitesides, G. M. *J. Am. Chem. Soc.* **1994**, *116*, 5057−5062.
(14) Boriack, P. A.; Christianson, D. W.; Kingery-Wood, J.; Whitesides, G. M. *J. Med. Chem.* **1995**, *38*, 2286−2291.
(15) Cappalonga Bunn, A. M.; Alexander, R. S.; Christianson, D. W. *J. Am. Chem. Soc.* **1994**, *116*, 5063−5068.
(16) Gilli, P.; Gerretti, V.; Gilli, G.; Borea, P. A. *J. Phys. Chem.* **1994**, *98*, 1515−1518.
(17) Williams, D. H.; Stephens, E.; O'Brien, D. P.; Zhou, M. *Angew. Chem., Int. Ed. Engl.* **2004**, *43*, 6596−6616.
(18) Lundquist, J. J.; Toone, E. J. *Chem. Rev.* **2002**, *102*, 555−578.
(19) Dunitz, J. D. *Chem. Biol.* **1995**, *2*, 709−712.
(20) Searle, M. S.; Westwell, M. S.; Williams, D. H. *J. Chem. Soc., Perkin Trans. 2* **1995**, 141−151.
(21) Ford, D. M. *J. Am. Chem. Soc.* **2005**, *127*, 16167−16170.
(22) Dill, K. A.; Bromberg, S. *Molecular Driving Forces: Statistical Thermodynamics in Chemistry & Biology*; Garland Science: New York, 2003.

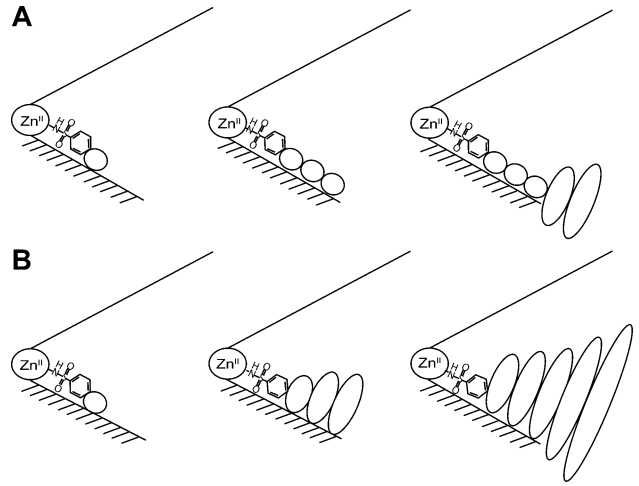

Figure 3. Two models for the interaction of the chains of arylsulfonamide ligands (containing one, three, and five residues) with the surface of carbonic anhydrase. This schematic represents the catalytic cleft of the enzyme as a cone with the Zn^{II} cofactor at the apex. The bottom surface (shaded) of the cleft is the "hydrophobic wall" of the enzyme. Schematic diagrams of (**A**) hydrophobic effect model and (**B**) interface mobility model. Ellipses diagrams depict the residues of the ligand; the sizes of the ellipses are roughly proportional to the mobility of the individual residues.

(because of the larger number of degrees of conformational freedom that were restricted to allow such an interaction to occur)[7] (Figure 3A).[13,15,23] We found it astonishing that *perfect* compensation was working with two very different types of chains, especially in light of the aforementioned experimental observation that increasing the length of the chain for *para*-substituted benzenesulfonamides with alkyl chains decreased the K_d.

Enthalpy/entropy compensation—the positive correlation between enthalpy and entropy of a physicochemical process as a variable of the system is modulated (that minimizes the variation of the free energy of binding)—is a phenomenon that is ubiquitous in biological systems[16−18] and has been discussed theoretically.[19−21] The qualitative explanation for enthalpy/entropy compensation centers on the inverse relationship between the amount of mobility ($\Delta S°$) at a protein−ligand interface and the strength of the interaction ($\Delta H°$) between the protein and the ligand at this interface.[17,20] Dunitz proposed a theoretical model for this phenomenon in which the protein−ligand complex is approximated as a potential energy well; the entropy of the complex can be estimated from the vibrational energy level spacing, which depends on the force constant of the well.[19] Assuming a Morse potential for the well, the force constant is proportional to the enthalpy of binding.[24] Using these approximations, the model generates an enthalpy/entropy compensation curve in which the entropy of the complex decreases monotonically with increasing exothermicity of complexation but becomes less sensitive to enthalpy when it is very favorable ($\Delta H° \leq -20$ kcal mol^{-1}). Although the model predicts a curved compensation curve, the compensation is roughly linear over small changes in enthalpy ($\Delta\Delta H° \leq 10$ kcal mol^{-1}). Thus, this theoretical model suggests an origin for the compensation between enthalpy and entropy on the basis of mobility of the protein−ligand complex. Williams and co-workers have provided experimental support for this idea of interfacial mobility by demonstrating that a glycopeptide dimer interface (a model for a protein−ligand interface) becomes tighter (the physical separation of monomers decreases) with increasing exothermicity of the dimerization.[17,25] The increasing exothermicity was compensated by an increasingly unfavorable entropy, which presumably reflected the decreasing mobility at the tighter dimer interface.

Isothermal titration calorimetry (ITC) is the premiere technique for separating free energy of binding into enthalpic and entropic components.[26] When the dissociation constant (K_d) is in the range of nanomolar to millimolar, this technique is able to measure the K_d and enthalpy of binding ($\Delta H°$) directly and the entropy of binding ($\Delta S°$) from the relation: $\Delta S° = (\Delta H° - \Delta G°)/T$.[26−28] Because ITC directly measures the heat released upon titration of the protein with the ligand, it avoids the artifacts of van't Hoff analysis arising from, for example, the temperature dependence of enthalpy of binding and/or of the change in specific heat capacity, the large errors in estimated parameters due to extrapolations from limited temperature ranges, and the thermal instability of proteins.[29−32]

In this paper, we have used ITC to separate the free energies of binding of the $ArEG_nOMe$ and $ArGly_nO^-$ ligands, as well as those of the previously uncharacterized $ArSar_nO^-$ series, into their enthalpic and entropic components. The objective of this work was to test our hypothesis of enthalpy/entropy compensation. Our intent was to characterize the interaction of these chains with the surface of BCA, to further our understanding of the interaction between these classes of chains and proteins. *Again*, *contrary* to our expectations, these calorimetric data clearly demonstrate that the enthalpy of binding becomes *less* favorable as the length of the chain increases, and the entropy of binding becomes *less un*favorable for all of the series studied. The changes in enthalpy and entropy of binding with chain length (total variation of 1−2 kcal mol^{-1} or 10−15%) perfectly compensate one another (making K_d insensitive to chain length) for all three series of ligands studied. On the basis of these data and of measurements of changes in heat capacities, we now rationalize the behavior of this system using a model in which the interface between the ligand and the hydrophobic wall of the protein becomes less intimate (less "tight") as the length of the chain increases (Figure 3B). The decreasing tightness of the interface (with increasing length of the chain) results in increasing mobility of the chain of the ligand in the complex

(23) Malham, R.; Johnstone, S.; Bingham, R. J.; Barratt, E.; Phillips, S. E. V.; Laughton, C. A.; Homans, S. W. *J. Am. Chem. Soc.* **2005**, *127*, 17061−17067.
(24) The Dunitz model implicitly assumes that the most probable bond length is independent of the depth of the well (enthalpy). Ford has recently called this assumption, and the resultant proportionality between enthalpy and force constant, into question (see ref 21).
(25) Calderone, C. T.; Williams, D. H. *J. Am. Chem. Soc.* **2001**, *123*, 6262−6267.
(26) Wiseman, T.; Williston, S.; Brandts, J. F.; Lin, L.-N. *Anal. Biochem.* **1989**, *179*, 131−137.
(27) Turnbull, W. B.; Daranas, A. H. *J. Am. Chem. Soc.* **2003**, *125*, 14859−14866.
(28) The lower limit of K_d (∼nM) arises from the sensitivity limit of the instrument. A protein concentration low enough to allow for a binding isotherm with some curvature (that is, not a step function) will not yield an adequate heat signal for binding reactions with values of K_d < nM. The upper limit (∼mM) arises from experimental issues (e.g., protein and/or ligand solubility, protein aggregation at high concentrations, etc.).
(29) Naghibi, H.; Tamura, A.; Sturtevant, J. M. *Proc. Natl. Acad. Sci. U.S.A.* **1995**, *92*, 5597−5599.
(30) Liu, Y. F.; Sturtevant, J. M. *Protein Sci.* **1995**, *4*, 2559−2561.
(31) Liu, Y. F.; Sturtevant, J. M. *Biophys. Chem.* **1997**, *64*, 121−126.
(32) These artifacts have contributed to belief in the scientific community that enthalpy/entropy compensation is often a statistical artifact. See, for example: Cornish-Bowden, A. *J. Biosci.* **2002**, *27*, 121−126. Houk, K. N.; Leach, A. G.; Kim, S. P.; Zhang, X. Y. *Angew. Chem., Int. Ed. Engl.* **2003**, *42*, 4872−4897.

and in decreasing magnitude of the unfavorable entropy of binding. In parallel, the decreasing tightness of the interface results in fewer van der Waals contacts between the ligand and protein and in decreasing exothermicity of binding.

These results provide a particularly well-defined example of enthalpy/entropy compensation. The binding of three series of oligomeric ligands, which are systematically varied by extending their chain length, with a model protein provides as simple a system as we know with which to examine enthalpy/entropy compensation. Understanding how to circumvent or to exploit this compensation is a key principle in the design of high-affinity ligands for proteins.[2,16]

Results

Synthesis of Ligands. $ArCO_2^-$ and ArCONHMe (Ar = *p*-$H_2NSO_2C_6H_4$−) were commercially available. We synthesized $ArGly_nO^-$, $ArEG_nOMe$, and $ArSar_1O^-$ (**1**, $n = 1-5$) as previously described.[13] Briefly, the ligands were synthesized by allowing the *N*-hydroxysuccinimidyl ester of *p*-carboxybenzenesulfonamide to react with the amino terminus of the appropriate oligomer. We synthesized $ArSar_nO^-$ (**1**, $n = 2-5$) through conventional solid-phase methods using the Fmoc protection strategy (see Experimental Section).

Validation of ITC: Measurement of Dissociation Constants. The concentration of BCA was determined by UV spectrophotometry.[33] High purity (≥95%) of the enzyme was ensured by capillary and gel electrophoresis,[8] and high activity (90−95%) of it was determined by the binding of ethoxzolamide (a selective, stoichiometric ligand that quenches the intrinsic fluorescence of Trp residues of CA when it binds[34,35]). The concentration of the ligand was determined by quantitative ^{1}H NMR (see Experimental Section). Turnbull and Daranas have recently demonstrated that the value of K_d estimated from curve fitting of ITC data is insensitive to the concentrations of the ligand and the protein (when the two are varied by 15%).[27] We discuss the influence of the concentrations of the ligand and the protein on the estimated enthalpy of binding and our analysis of error for all thermodynamic parameters in the next section. ITC provides the stoichiometry of binding as a fitting parameter; this experimental parameter serves as an internal check on the relative accuracy of the concentrations of the protein and the ligand. These stoichiometries were 1.00 ± 0.05 for all of the ligands studied here; they validate our methods to estimate the concentrations of both components.

Figure 4 shows a representative thermogram from ITC with the associated curve fitting.[26] The dissociation constants from the fitting procedure for $ArEG_nOMe$ and $ArGly_nO^-$ are in good agreement with those we reported previously[13] (Table 1); these earlier values of K_d were obtained using a fluorescence competition assay and are thus independent. The agreement between the two validates both the ITC methodology and the values of K_d. We have confirmed the previously reported insensitivity of K_d to chain length (n) for $ArGly_nO^-$ ($K_d \sim 0.23$ μM) and $ArEG_nOMe$ ($K_d \sim 0.10$ μM) and have reported for the first time that the $ArSar_nO^-$ series also exhibits this insensitivity of K_d to chain length ($K_d \sim 0.40$ μM) (Figure 5A).

Analysis of Experimental Uncertainty. Several authors have advised caution in the interpretation of thermodynamic results (particularly enthalpy/entropy compensation relationships) because of random errors in the estimation of the enthalpy and entropy of binding.[32] Thus, we carried out a careful analysis of error.

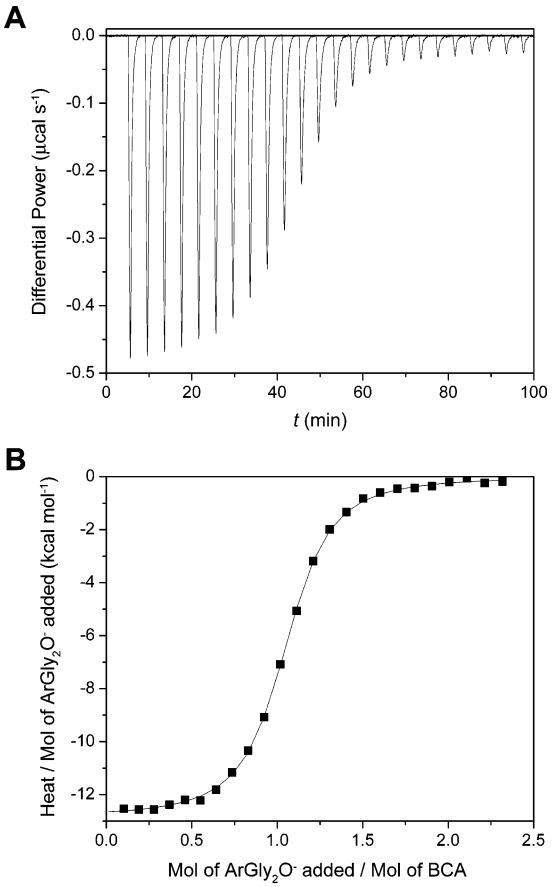

Figure 4. Representative ITC experiment showing the titration of an arylsulfonamide ligand into a solution of bovine carbonic anhydrase II (BCA). The sample cell contained 10.0 μM BCA in 20 mM sodium phosphate buffer, pH 7.5, and 0.6% DMSO-d_6 (v/v) (to solubilize the arylsulfonamide and to allow for NMR quantitation; see Experimental Section). The injection syringe contained 103 μM $ArGly_2O^-$ (**1**) in the same buffer. One injection of 2.0 μL preceded 24 injections of 12.0 μL. The interval between injections was 4 min. (**A**) Data after baseline correction. (**B**) Data after peak integration, blank subtraction, and normalization to moles of injectant. The solid line shows a sigmoid fit to a single-site binding model (with the first datum omitted). The dissociation constant ($K_d = 0.20$ μM), enthalpy of binding ($\Delta H° = -12.6$ kcal mol^{-1}), and stoichiometry of binding ($N = 1.02$) were the fitting parameters in the analysis. See Experimental Section for details.

In ITC, the heat released upon titration of one binding partner with another is normalized to the number of moles of titrant added (Figure 4B). Thus, the estimated value of $\Delta H°$ is inversely proportional to the concentration of the titrant (here, the arylsulfonamide) because the quantity of titrant added is proportional to the concentration of the titrant. For this reason, fractional errors in the estimated value of $\Delta H°$ are almost equal to fractional errors in the estimation of concentration of the arylsulfonamide.[27] Errors in the concentration of the component in the sample cell (here, BCA) do not affect the estimated value of $\Delta H°$[27] but are instead reflected in deviations of the binding stoichiometry from unity (see previous section). To reduce the uncertainty in concentration of the ligand, we used quantitative ^{1}H NMR to estimate this concentration relative to maleic acid as an internal standard. We assumed an uncertainty of 3% from

(33) Nyman, P. O.; Lindskog, S. *Biochim. Biophys. Acta* **1964**, *85*, 141−151.
(34) Chen, R. F.; Kernohan, J. C. *J. Biol. Chem.* **1967**, *242*, 5813−5823.
(35) Kernohan, J. C. *Biochem. J.* **1970**, *120*, 26P.

Table 1. Thermodynamic Parameters for the Binding of Arylsulfonamide Ligands (of Structure **1**) to Bovine Carbonic Anhydrase II (BCA) in 20 mM Sodium Phosphate, pH 7.5, with 0.6% (v/v) DMSO-d_6 at 298 K

ligand	n	K_d μM	lit. K_d[a] μM	$\Delta H°$ kcal mol^{-1}	$\Delta S°$ cal mol^{-1} K^{-1}	ΔC_p cal mol^{-1} K^{-1}
$ArCO_2^-$	–	0.50 ± 0.02	0.27[b]	−14.8 ± 0.5	−21.0 ± 1.5	–
ArCONHMe	–	0.20 ± 0.01	0.083[c]	−10.8 ± 0.4	−5.5 ± 1.5	–
$ArEG_nOMe$	1	0.068 ± 0.004	0.10[d]	−10.2 ± 0.5	−1.5 ± 1.5	−40 ± 8
	2	0.085 ± 0.005	0.13[d]	−10.0 ± 0.3	−1.3 ± 1.0	–
	3	0.10 ± 0.01	0.16[d]	−10.0 ± 0.3	−1.4 ± 1.0	−47 ± 8
	4	0.12 ± 0.01	0.21[d]	−9.4 ± 0.3	+0.1 ± 1.0	–
	5	0.13 ± 0.01	0.21[d]	−9.0 ± 0.3	+1.3 ± 1.0	−40 ± 20
$ArGly_nO^-$	1	0.26 ± 0.01	0.30[d]	−13.3 ± 0.4	−14.6 ± 1.4	−24 ± 2
	2	0.20 ± 0.01	0.26[d]	−12.9 ± 0.4	−12.5 ± 1.3	–
	3	0.23 ± 0.01	0.33[d]	−12.3 ± 0.4	−10.9 ± 1.4	−18 ± 10
	4	0.25 ± 0.01	0.37[d]	−11.5 ± 0.4	−8.4 ± 1.2	–
	5	0.29 ± 0.02	0.37[d]	−11.1 ± 0.5	−7.3 ± 1.8	−20 ± 7
$ArSar_nO^-$	1	0.62 ± 0.03	–	−11.7 ± 0.4	−10.7 ± 1.2	−43 ± 10
	2	0.30 ± 0.01	–	−11.5 ± 0.4	−8.8 ± 1.2	–
	3	0.34 ± 0.01	–	−10.4 ± 0.4	−5.4 ± 1.2	−45 ± 16
	4	0.41 ± 0.02	–	−10.0 ± 0.4	−4.4 ± 1.3	–
	5	0.45 ± 0.02	–	−9.5 ± 0.3	−2.9 ± 1.0	−49 ± 23

[a] Literature values of dissociation constants for the binding of arylsulfonamides to BCA or human carbonic anhydrase II (HCA). [b] Measured with HCA in: Taylor, P. W.; King, R. W.; Burgen, A. S. V. *Biochemistry* **1970**, *9*, 2638−2645. [c] Measured with HCA in ref 11. [d] Measured with BCA in ref 13.

this method of quantitation from literature reports.[36] To arrive at an uncertainty for values of $\Delta H°$, we propagated the error in concentration of the ligand (taken as 3% of the estimated value of $\Delta H°$) with the largest variation of an individual experiment from the mean value of two to four replicate measurements of $\Delta H°$, assuming that the error in concentration of the ligand and the error in measurement were independent.

For errors in values of K_d for all of the ligands, we used the maximum variation of an individual measurement from the mean of two to four replicate measurements. Errors in values of $\Delta S°$ were estimated by propagating the errors in values of $\Delta H°$ and K_d, assuming that the two errors were independent. Changes in heat capacity (ΔC_p) were determined by measuring $\Delta H°$ as a function of temperature over the range $T = 288-308$ K (see section on Changes in Heat Capacity). Errors in values of ΔC_p were estimated by the errors in slopes of linear plots of $\Delta H°$ vs T that were given by the least-squares fitting procedure.

Table 1 gives the measured thermodynamic parameters with their associated uncertainties.

Trends in Enthalpy and Entropy Were *Opposite* to Those We Expected. We predicted that as the chain of the ligand became longer (i.e., as n increased), $\Delta H°$ would become more favorable (because of increasing area of contact between the chain and the hydrophobic wall of the enzyme) and $T\Delta S°$ would become more unfavorable (because of entropic restrictions to the motion of the chain resulting from proximity to the wall).[23] The result that we observed was counter to this hypothesis: $\Delta H°$ became less favorable and $T\Delta S°$ became less unfavorable, with increasing chain length (Figure 5B,C). It is especially remarkable that we observe the same counterintuitive result for three, structurally different chains; this similarity gives us confidence that the result is correct and not an artifact.

This result poses the central conundrum of this paper: why does the enthalpy of interaction of the chains become less favorable, and the entropy less unfavorable, as the chain becomes longer? We discuss the experimental results in the following sections and then present two possible models to rationalize the data in the Discussion section.

No Clear Discontinuity in Thermodynamic Properties When the Chain Exceeds the Presumed Length of the Hydrophobic Wall of the Enzyme. There was no discontinuity in plots of $\Delta H°$ and $T\Delta S°$ with chain length (n) for any of the series of ligands (Figure 5B and 5C) when the length of the chain exceeded the depth of the conical cleft (15 Å, $n \sim 2-3$) of BCA (Figure 2).[14,15] The plots were linear (within error) over the length studied and did not meet our initial expectation that $\Delta H°$ and $T\Delta S°$ would plateau once there were a sufficient number of residues in the chain for additional residues to be outside the active site. This result suggests that there is still an interaction of the chain with BCA when $n > 3$ and that this interaction is similar for residues in ligands with short ($n < 3$) chains and for those in ligands with long ($n \geq 3$) chains.

This finding seems incompatible with evidence describing binding of $ArGly_nO^-$ to BCA as measured by NMR relaxation times. These data indicated that values of T_2 (120 ms) of residues separated by more than three residues from the phenyl ring were significantly larger than those ($T_2 < 25$ ms) of the three residues closest to the phenyl ring; this result suggests a small amount of interaction of these distal residues with the protein.[13] There was a difference between T_2 for these residues farther from the phenyl ring and T_2 (230 ms) for residues of the free, uncomplexed ligand; there is, thus, apparently *some* interaction with BCA of the residues farther than three residues from the phenyl ring.

Molecular dynamics simulations indicated that the benzyl ester in $ArGly_3OBn$ (the benzyl moiety is in a similar position in this ligand as the fourth and fifth residues of $ArGly_5O^-$) and the pendant amino acid in $ArEG_3NHR$ (R = Gly, Phe) could both interact with the surface of CA in certain conformations of the ligands.[37,38] These simulations, thus, support the calorimetric data and suggest a possible interaction with CA of residues farther than three residues from the phenyl ring.

We believe that there is an interaction with the protein of residues of $ArGly_nO^-$ and $ArEG_nOMe$ (and also $ArSar_nO^-$) where $n \geq 3$. We cannot, however, discriminate between the

(36) Maniara, G.; Rajamoorthi, K.; Rajan, S.; Stockton, G. W. *Anal. Chem.* **1998**, *70*, 4921−4928.
(37) Chin, D. N.; Whitesides, G. M. *J. Am. Chem. Soc.* **1995**, *117*, 6153−6164.
(38) Chin, D. N.; Lau, A. Y.; Whitesides, G. M. *J. Org. Chem.* **1998**, *63*, 938−945.

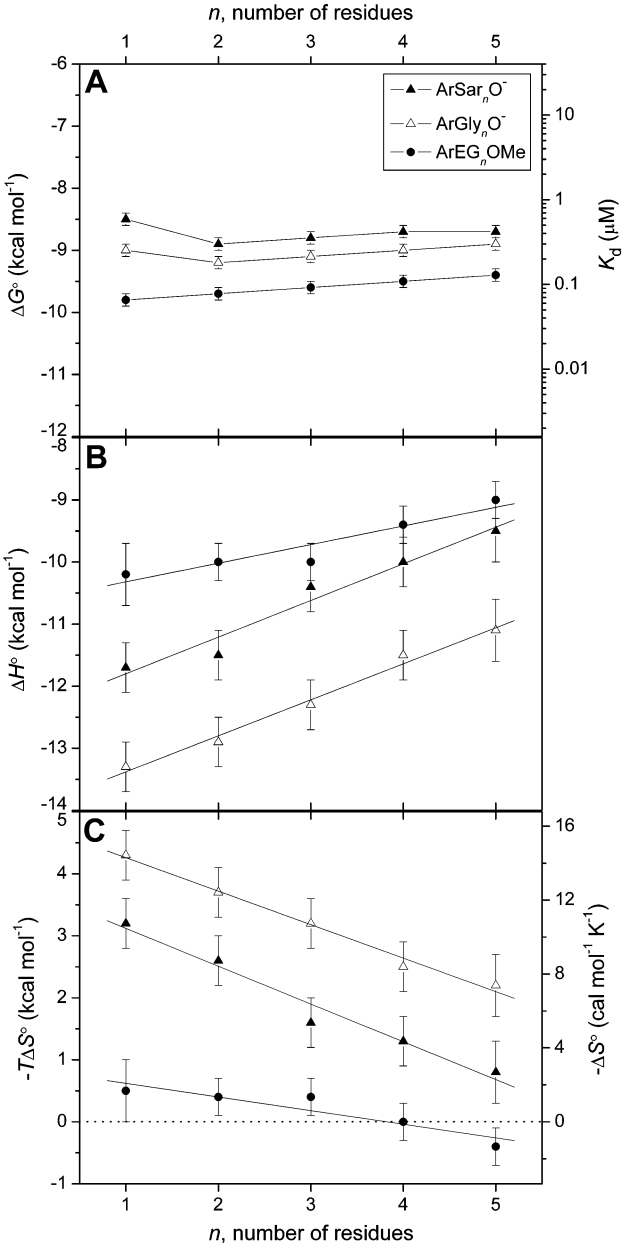

Figure 5. Variation in (**A**) free energy of binding and dissociation constant, (**B**) enthalpy of binding, and (**C**) entropy of binding with the number of residues in the chain for arylsulfonamide ligands of structure **1**. Error bars are discussed in the text (see Results section). Linear fits to the data in (**B**) and (**C**) are shown. The observed fitting parameters (slope in kcal mol^{-1} residue^{-1}, *y*-intercept in kcal mol^{-1}) are as follows: for (**B**), ArGly$_n$O$^-$ (0.58 ± 0.04, -14.0 ± 0.1), ArSar$_n$O$^-$ (0.59 ± 0.07, -12.4 ± 0.2), ArEG$_n$OMe (0.30 ± 0.06, -10.6 ± 0.2); for (**C**), ArGly$_n$O$^-$ (-0.54 ± 0.03, 4.8 ± 0.1), ArSar$_n$O$^-$ (-0.61 ± 0.06, 3.7 ± 0.2), ArEG$_n$OMe (-0.22 ± 0.05, 0.8 ± 0.2). Uncertainties were given by the linear least-squares fitting procedure. The horizontal dashed line in (**C**) separates favorable ($-T\Delta S° < 0$) from unfavorable ($-T\Delta S° > 0$) entropy of binding.

interactions with CA of residues close to the ring ($n < 3$) and those farther from the ring ($n > 3$) on the basis of thermochemistry.

Similar Interactions of Oligoglycine (Gly$_n$), Oligosarcosine (Sar$_n$), and Oligoethylene Glycol (EG$_n$) Chains with the Hydrophobic Wall of CA. Qualitatively, the trends for both $\Delta H°$ and $T\Delta S°$ with chain length (n) for the ArGly$_n$O$^-$, ArSar$_n$O$^-$, and ArEG$_n$OMe ligands roughly parallel one another (Figure 5B,C). To assess these trends quantitatively, we

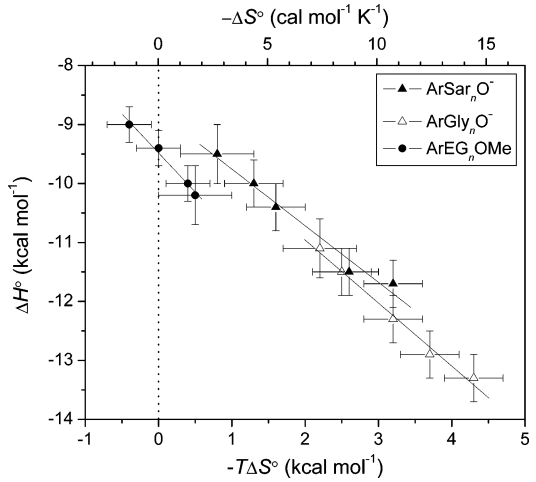

Figure 6. Enthalpy/entropy compensation plot: variation of the enthalpy of binding with the entropy of binding for ligands of structure **1** with $n \geq 1$. Error bars are as in Figure 5. The solid lines are linear fits to the data sets, and their slopes give the following values for compensation: -0.96 ± 0.08 (ArSar$_n$O$^-$), -1.07 ± 0.07 (ArGly$_n$O$^-$), and -1.32 ± 0.09 (ArEG$_n$OMe). Uncertainties were given by the linear least-squares fitting procedure. The dotted vertical line separates favorable ($-T\Delta S° < 0$) from unfavorable ($-T\Delta S° > 0$) entropy of binding.

constructed linear fits to the plots; the slopes were similar for all three series. The similarity in slopes of the series suggests that the three chains interact similarly with the surface of BCA.

Although the best-fit lines of $\Delta H°$ (and $-T\Delta S°$) to chain length (n) for the three series were roughly parallel (i.e., they had similar slopes), they were off-set (i.e., they had different *y*-intercepts). These different *y*-intercepts reflect differences in $\Delta H°$ and $-T\Delta S°$ among the three series that depend on the nature of the first residue (the residue adjacent to the phenyl ring). The addition of subsequent ($n > 1$) residues (either Gly, Sar, or EG) changes the thermodynamics of binding by roughly the same amount (because the slopes of the best-fit lines were the same). These results suggest that the interactions with the hydrophobic wall of CA of Gly$_n$, Sar$_n$, and EG$_n$ chains (beyond the first residue) are thermodynamically similar.

Plots of $\Delta H°$ vs $T\Delta S°$ (enthalpy/entropy compensation plots) for the three series have slopes near unity and thus show almost perfect compensation between $\Delta H°$ and $T\Delta S°$ (Figure 6).

Information about Buried Molecular Surface Area from Changes in Heat Capacity (ΔC_p). The change in heat capacity (ΔC_p) has been termed the "signpost" for the hydrophobic effect; it is negative for the association of hydrophobic molecules in water.[22,39] Models of protein−ligand binding have been proposed that correlate ΔC_p with buried molecular surface area (both polar and nonpolar).[40−42] Sturtevant[43] has discussed additional contributions to ΔC_p upon protein−ligand complexation: positive contributions (hydrogen-bond formation, increase in number of vibrational modes of the protein from relaxing of the structure), negative contributions (exposure of electrostatic charges, reduction in number of vibrational modes of the protein from stiffening of the protein), and neutral contributions

(39) Southall, N. T.; Dill, K. A.; Haymet, A. D. J. *J. Phys. Chem. B* **2002**, *106*, 521−533.
(40) Livingstone, J. R.; Spolar, R. S.; Record, M. T. *Biochemistry* **1991**, *30*, 4237−4244.
(41) Spolar, R. S.; Record, M. T. *Science* **1994**, *263*, 777−784.
(42) Murphy, K. P.; Freire, E. *Adv. Protein Chem.* **1992**, *43*, 313−361.
(43) Sturtevant, J. M. *Proc. Natl. Acad. Sci. U.S.A.* **1977**, *74*, 2236−2240.

(conformational mobility from, for instance, an increase in the number of accessible conformations).

We measured changes in heat capacity (ΔC_p) for $n = 1$, 3, and 5 for the different series to clarify the nature of the interactions of these chains with BCA. We measured the variation of $\Delta H°$ with temperature over the range 288−308 K[44] and used the definition of ΔC_p in eq 1, where T is the temperature in K and $\Delta H°(T)$ is the enthalpy of binding at temperature T.

$$\Delta C_p(T) = \left(\frac{\partial \Delta H°(T)}{\partial T}\right)_p \quad (1)$$

Assuming a constant change in heat capacity over this temperature range, this relation simplifies to eq 2, where $\Delta H°(0)$ is the enthalpy of binding at $T = 0$ K.

$$\Delta H°(T) = T\Delta C_p + \Delta H°(0) \quad (2)$$

Simple linear regression of eq 2 affords ΔC_p.

We titrated the ligand with protein under conditions in which >99.5% of the added protein would be bound by the ligand to obtain an estimate of $\Delta H°$ from a single injection. We averaged at least seven injections and determined uncertainties (standard deviations of these injections) of <0.2 kcal mol^{-1} (see Experimental Section for further information). Table 1 lists values for ΔC_p obtained from linear fits to these data. The values of ΔC_p are small, do not vary with chain length within each series, and vary only slightly among the series. For benzenesulfonamide, ΔC_p has been reported to be +25 cal mol^{-1} K^{-1}.[45] These results suggest that ΔC_p is dominated by the benzenesulfonamide group with some influence of the first residue of the chain.

At first glance, these results seem to contradict a model in which the chains of the ligand interact hydrophobically with the surface of BCA (ΔC_p should become more negative with increasing chain length in such a model). In the next section, we explore contributions to ΔC_p (listed at the beginning of this section) that could rationalize the data with such a model. We also introduce another theoretical model and discuss its compatibility with the experimental data.

Discussion

Two Possible Thermodynamic Models. We can imagine two possible models that are consistent with the trends of $\Delta H°$ and $-T\Delta S°$ with chain length (Figure 5): (i) one based on hydrophobic interactions (Figure 3A) and (ii) one based on interfacial mobility (mobility of the protein−ligand interface) (Figure 3B). We conclude that the second model is the only one consistent with the experimental data.

Overview of the Hydrophobic Effect Model. The model based on hydrophobic interactions (Figure 3A) postulates that the interaction of Gly_n, Sar_n, and EG_n chains with CA is due to the classical hydrophobic effect,[22,39] the association of hydrophobic molecules in aqueous solution. At temperatures near 298 K, the hydrophobic effect occurs with a favorable entropy ($-T\Delta S° < 0$) and a negligible enthalpy ($\Delta H° \sim 0$). This model rationalizes the data by proposing that as the chain of the ligand gets longer the amount of nonpolar surface area that becomes buried upon complexation increases; this increasing buried surface area is manifested as a favorable contribution to $-T\Delta S°$. For this hypothesis to explain the data, the contribution of the hydrophobic effect to the observed $T\Delta S°$ must be greater than the unfavorable contribution of restricting the modes of motion of the chain. In this model, the decreasing magnitude of $\Delta H°$ (decreasing exothermicity) with increasing chain length could have several origins: (i) loss of hydrogen bonds between the unassociated form of the ligand (or of the protein) upon complexation, (ii) unfavorable conformations (e.g., eclipsed bonds) of the chain in the complex, and/or (iii) destabilization of placing a lone pair of electrons on the chain into contact with the hydrophobic wall of CA. We discuss below how none of these possibilities can adequately explain the trend of $\Delta H°$ with chain length for the three series of ligands.

Overview of the Interfacial Mobility Model. The second possible model (interfacial mobility model) (Figure 3B) postulates that the interface between the protein and the chain of the ligand becomes "looser" (less tight) with increasing chain length. This decreasing tightness of the interface is reflected in a less unfavorable $T\Delta S°$ (due to greater mobility of the chain) and a correspondingly less favorable $\Delta H°$ (due to fewer van der Waals contacts between the protein and the ligand) as the length of the chain increases. Enthalpy and entropy perfectly compensate, and there is no change in the observed K_d.

In this model, the decreasing tightness of the interface arises because more distal residues (those farther from the phenyl ring) of the chain destabilize the binding of the more proximal residues (those closer to the phenyl ring). To explain the data, this model requires that residues that are bound "tightly" in ligands with a short chain be destabilized by more distal residues in ligands with a long chain; if these distal residues did not interact with more proximal residues of the chain or with the protein (and were oriented into solution), $\Delta H°$ and $T\Delta S°$ would become independent of chain length at that point.

Residues that are farther (more distal) from the phenyl ring are plausibly more mobile than those that are closer (more proximal) to the ring. The conical catalytic cleft of CA could force a destabilizing interaction (e.g., torsional or steric strain) of these mobile, distal residues with the bound form of more proximal residues. The protein−ligand complex would relax to a more stable state in which the destabilization is alleviated, by decreasing the tightness of the interface between the more proximal residues and the cleft of CA. The thermodynamics discussed above would then follow.

Evaluation of Both Models in Light of the Experimental Data. Because both models can adequately explain the trends in entropy (and, to a lesser extent, in enthalpy) with chain length, we consider their ability to explain the remaining thermodynamic data. We consider both models, in turn, with respect to the following experimental observations: (i) the chain-length independence of ΔC_p, (ii) the decreasing magnitude of $\Delta H°$ (decreasing exothermicity) with increasing chain length, (iii) the similar trends of $\Delta H°$ and $-T\Delta S°$ with chain length for the different series of ligands, and (iv) the lack of a discontinuity in plots of $\Delta H°$ and $-T\Delta S°$ with chain length. We first consider the "hydrophobic effect" model (Figure 3A); we conclude that this model is inconsistent with these data.

(44) BCA has been shown to be stable over this temperature range. See: Matulis, D.; Kranz, J. K.; Salemme, F. R.; Todd, M. J. *Biochemistry* **2005**, *44*, 5258−5266.
(45) Binford, J. S.; Lindskog, S.; Wadsö, I. *Biochim. Biophys. Acta* **1974**, *341*, 345−356.

Hydrophobic Effect Model Is Inconsistent with the Thermodynamic Data. First, ΔC_p was independent of chain length for all three series of ligands; the hydrophobic effect model predicts that ΔC_p would depend on the amount of buried molecular surface area (and thus, on chain length). The correlation between ΔC_p and buried molecular surface area of Spolar and Record[41] is given in eq 3a, and that of Murphy and Freire[42] is given in eq 3b:

$$\Delta C_p = 0.32\Delta A_{np} - 0.14\Delta A_p \quad (3a)$$

$$\Delta C_p = 0.45\Delta A_{np} - 0.26\Delta A_p \quad (3b)$$

where ΔA_{np} is the change in nonpolar surface area upon protein−ligand complexation ($\Delta A_{np} < 0$ for the burial of surface area upon complexation) and ΔA_p is the change in polar surface area. We discuss the $ArGly_nO^-$ ligands in detail because there are X-ray crystal structures and NMR relaxation data for CA−ligand complexes of this series.[13,15] We expect that the conclusions regarding the validity of this model drawn from $ArGly_nO^-$ will be applicable to $ArSar_nO^-$ and $ArEG_nOMe$ because all of the ligands behave similarly in the thermodynamics of their interactions with BCA (Figure 5).

Given the surface area buried by each Gly residue from the X-ray crystal structures (49 Å^2 Gly^{-1})[15] and assuming that the entire interface was nonpolar (as observed in the X-ray crystal structure),[15] we would expect a difference in ΔC_p between $ArGly_3O^-$ and $ArGly_1O^-$ to be in the range of −31 to −44 cal mol^{-1} K^{-1} (from eqs 3a and 3b, respectively). Even with the errors of the data, the experimentally observed difference (+6 ± 12 cal mol^{-1} K^{-1}) was much larger than this value and of opposite sign. A difference in $\Delta C_p \sim 0$ can be obtained if a significant fraction of the buried surface area was polar (although the CA−Gly interface was completely nonpolar in the X-ray crystal structure[15]). Polar surface area at the interface would provide a positive contribution to ΔC_p (from eqs 3a and 3b, respectively); a difference of $\Delta A_p = -68$ to -62 Å^2 ($\Delta A_{np} = -30$ to -36 Å^2) between $ArGly_3O^-$ and $ArGly_1O^-$ yields $\Delta\Delta C_p \sim 0$ for $\Delta\Delta A_{np} + \Delta\Delta A_p = -98$ Å^2 (eq 3). Spolar and Record[41] have proposed eq 4 to relate the buried nonpolar surface area with the entropy of binding from hydrophobic effect contacts ($\Delta S°_{HE}$) (at $T = 298$ K):

$$\Delta S°_{HE} = -0.083\Delta A_{np} \quad (4)$$

Using the larger (in magnitude) value for the difference in ΔA_{np} of −36 Å^2 (from eq 3b) gives a difference in $\Delta S°_{HE}$ of $\sim +3.0$ cal mol^{-1} K^{-1} between $ArGly_3O^-$ and $ArGly_1O^-$. This value is close to the experimentally observed difference in $\Delta S°$ of +3.7 cal mol^{-1} K^{-1} (Table 1), but this experimentally observed value must also take into account the conformational restriction of the additional rotors in two Gly residues between $ArGly_3O^-$ and $ArGly_1O^-$ ($\Delta S°_{conf} \sim -9$ cal mol^{-1} K^{-1}).[2,7] Thus, $\Delta S°_{HE}$ must be greater than $\Delta S°$ by ~9 cal mol^{-1} K^{-1}; this model is inconsistent with the data from ΔC_p.

Second, the hydrophobic effect model cannot explain compellingly why $\Delta H°$ decreases in magnitude (becomes less favorable) with increasing chain length (n). van der Waals contacts, which the interactions between Gly and the hydrophobic wall of CA seem to be, are expected to be favorable enthalpically and should make a favorable contribution to $\Delta H°$ that increases with chain length.[22,23,46] Unfavorable conformations of the different chains in the CA−ligand complex seem unlikely, given the flexible nature of the chains[47] and the lack of eclipsed or other unfavorable conformations in the crystal structure.[14,15] The removal of hydrogen bonds either within (intramolecular) or between (intermolecular) ligand molecules upon complexation with the enzyme could explain the trend of $\Delta H°$ with chain length. We would not, however, expect such hydrogen bonds to be present in the uncomplexed ligand because the chains we studied were short and flexible, and the high dielectric constant of the aqueous buffer should disfavor such weak, electrostatic interactions.[22] Further, it strains coincidence that the amount and/or strength of bonding (within or between) uncomplexed ligand molecules would be the same for the different chains studied or that the unfavorable conformations of the chains would be unfavorable by the same amount for the different chains (possibilities that are required to explain the similar variation of $\Delta H°$ with chain length for the different series, see Figure 5).

Third, we consider the most perplexing issue with this model: its inability to explain why there were similar trends in plots of $\Delta H°$ and $-T\Delta S°$ with chain length for the three different types of chains (Figure 5A,B). For instance, sarcosine has more hydrophobic surface area than glycine because of the N−Me substituent but behaves similarly thermodynamically. Ethylene glycol is very different structurally than either of the peptidyl chains but, again, behaves similarly.

Finally, the observation that residues that extend past the conical cleft of BCA (residues beyond the third one) and are oriented into solution, as evidenced by X-ray crystal structures[14,15] (Figure 2) and NMR relaxation[13] data, still exert the same influence on the thermodynamics of binding as residues that directly interact with the hydrophobic wall of the enzyme is incompatible with this model. There is no plateau (or discontinuity) in plots of $\Delta H°$ or $-T\Delta S°$ with chain length that would be predicted from this model (Figure 5).

Interfacial Mobility Model Is Consistent with the Thermodynamic Data. We now consider the interfacial mobility model (Figure 3B) in the context of the four pieces of experimental data; we believe that this model is compatible with the data. First, the independence of ΔC_p on chain length within each series and the modest variation of ΔC_p among the series are readily explained by this model: ΔC_p is dominated by the benzenesulfonamide group with some influence from the first residue of the chain. Subsequent residues ($n > 1$) interact weakly with the hydrophobic wall of the enzyme and do not influence ΔC_p.

Second, as discussed above, the interfacial mobility model can explain the observation that $\Delta H°$ becomes less favorable (less exothermic) as chain length increases.

(46) Vondrasek, J.; Bendova, L.; Klusak, V.; Hobza, P. *J. Am. Chem. Soc.* **2005**, *127*, 2615−2619.
(47) Ostuni, E.; Chapman, R. G.; Holmlin, R. E.; Takayama, S.; Whitesides, G. M. *Langmuir* **2001**, *17*, 5605−5620.

Third, this model can explain the similar trends of both $\Delta H°$ and $-T\Delta S°$ with chain length of the different series of ligands. In this model, these similar trends (Figure 5) are due to similar destabilization of the binding of residues of the chain by more distal residues (those farther from the phenyl ring). This effect could arise because the constrained orientation of the conical cleft of the enzyme forces the mobility of the distal residues of the chain to destabilize the binding of more proximal residues through, for example, steric or torsional strain. The complex then relaxes by decreasing the tightness of the interface between the more proximal residues of the chain and the hydrophobic wall of CA. This observation does not require that the chains interact directly with the hydrophobic wall of CA in a similar manner (consistent with the different structures and flexibilities of these chains).

Finally, the interfacial mobility model can explain why residues that extend past the presumed length of the wall (those farther than three residues from the phenyl ring, $n > 3$) can still affect the thermodynamics of interaction. This model can rationalize this observation because these residues, which do not directly interact with the wall, can still destabilize the bound form of more proximal residues that do interact with the wall. A direct interaction of these residues (where $n > 3$) with the enzyme is not required in this model. We anticipate that the thermodynamic parameters of interaction ($\Delta H°$ and $T\Delta S°$) will plateau when the chain is sufficiently long that additional destabilization of the binding of more proximal residues (that do interact with the wall) by more distal ones cannot occur; this required length would seem to be greater than that of the ligands studied here ($n = 5$). The interfacial mobility model (Figure 3B) is, thus, consistent with all of the experimental data.

Mechanism of the Interfacial Mobility Model Is Unclear. The exact mechanism of the interfacial mobility model remains unclear. Although we have presented the model as involving destabilization of the binding of residues of the chain by more distal residues, the model could involve destabilization in the protein itself as a result of binding of the ligand. Williams and co-workers have recently discussed how enthalpy/entropy compensation could originate from a loosening of protein structure that is coupled to ligand binding.[17,48,49] Ligands with long chains could destabilize interactions within the protein itself (perhaps through a weakening of hydrogen bonds in the protein in a process that does not require gross conformational changes in the structure of the protein). We have no evidence for or against this model and so cannot comment on the contribution of it, if any, to our system.

Conclusions

This paper establishes that ligands with oligosarcosine chains exhibit the same insensitivity of K_d to chain length as the previously reported oligoglycine- and oligoethylene glycol-containing ligands. We have dissected the thermodynamics of binding of these three series of ligands. Although we anticipated that the enthalpy of binding would become more favorable with increasing chain length and that the entropy of binding would become more unfavorable,[23] the results were exactly opposite to these expectations. That is, increasing the chain length (number of residues) of these ligands monotonically reduced the favorable enthalpy of binding and decreased the entropic cost of binding. Surprisingly, the different chains seem to behave as slight variations on a general theme with similar variations of enthalpy and entropy with chain length. Our results have thus revealed an unexpected example of enthalpy/entropy compensation in these structurally unrelated chains. We have proposed a model that explains these data. This model requires that the mobility of the chain of the ligand in the protein−ligand complex increases with increasing chain length and that there be an active destabilization of the binding of residues of the chain that are closer to the phenyl ring by residues of the chain that are farther from the phenyl ring (Figure 3B).

A common approach to rational drug design invokes the principle of additivity: the thermodynamics of binding of a ligand to a protein are assumed to be equal to the sum of the thermodynamics of binding of the individual components of the ligand (with an appropriate entropic benefit of linking the different components together).[17,50−53] Williams and co-workers have discussed a complication to this approach by the concept of "negative cooperativity"; an interface that displays negative cooperativity is one in which the multiple interactions between a ligand and a protein are mutually incompatible.[17,48,49] At a negatively cooperative interface, the enthalpy of binding is less favorable, and the entropy of binding is less unfavorable, in the combined interaction than in the separate, individual interactions.[2] Our results suggest an even more extreme situation than negative cooperativity: the enthalpy of the combined interaction can be not only less favorable than the sum of the independent interactions, but also less favorable than even one of the interactions. According to our model (Figure 3B), this less favorable total enthalpy is due to destabilization of one of the interactions by another. Our results, thus, demonstrate that an additive approach can reach completely incorrect conclusions because of this influence of one component (interaction) on the binding of another.

One of the guiding principles in rational drug design has been the design of ligands that fill the active site of an enzyme to increase the number of interactions between the protein and the ligand.[51] Our results suggest that appending substituents to a parent ligand in an attempt to increase affinity for a target receptor might actually be deleterious for the enthalpy of binding because of the destabilization of the binding of the parent ligand to the enzyme by the appended moiety (as opposed to simple steric strain between the appended moiety and the protein). Although in our case, the free energy of binding is not affected by the added groups (the longer chains), it is possible that in certain cases a smaller, more carefully designed ligand might bind with a lower free energy of binding to a target protein than a larger ligand (even one that does not merely encounter steric repulsion with residues of the active site of the protein).

One of the tenets in the design of multivalent ligands has been to avoid flexible (conformationally mobile) linkers because of the high cost in conformational *entropy* that would occur on complexation (Figure 1). Our results suggest that flexible linkers might also be disadvantageous from an *enthalpic* standpoint

(48) Williams, D. H.; Stephens, E.; Zhou, M. *J. Mol. Biol.* **2003**, *329*, 389−399.
(49) Williams, D. H.; O'Brien, D. P.; Sandercock, A. M.; Stephens, E. *J. Mol. Biol.* **2004**, *340*, 373−383.
(50) Jencks, W. P. *Proc. Natl. Acad. Sci. U.S.A.* **1981**, *78*, 4046−4050.
(51) Gohlke, H.; Klebe, G. *Angew. Chem., Int. Ed. Engl.* **2002**, *41*, 2645−2676.
(52) Andrews, P. R.; Craik, D. J.; Martin, J. L. *J. Med. Chem.* **1984**, *27*, 1648−1657.
(53) Böhm, H. J. *J. Comput.-Aided Mol. Des.* **1994**, *8*, 243−256.

because the linker (or chain) could destabilize the interaction of the ligand with the protein (relative to the ligand lacking the chain or linker). Our model (Figure 3B) predicts that rigid linkers would be able to avoid this enthalpic destabilization because of their reduced mobility, which is the origin of the destabilization between residues of the chain. This hypothesis remains to be tested.

The lowest free energy for the CA/arylsulfonamide complexes is achieved by optimizing the entropy (mobility) of the system at the expense of the enthalpy (fewer van der Waals contacts). We find it surprising that an alternative solution in which the magnitude of the enthalpy is optimized (more van der Waals contacts by increasing the tightness of the interface) at the expense of the entropy (lower conformational mobility) is apparently not available to the system. We cannot address the issue of whether the preference for optimization of entropy is directed by the catalytic cleft (or other structural aspects) of CA or is an innate property of the interaction of these types of chains with hydrophobic patches.

The most surprising result from our investigation is the near perfect compensation between enthalpy and entropy (Figure 6) for the three series of ligands. At this stage, we do not understand clearly and intuitively why the significant changes in enthalpy (with chain length) are perfectly balanced by changes in entropy. The fact that we observe this compensation for three different series of ligands suggests that it is a general phenomenon (at least within these series). It could, therefore, characterize weak interactions of other types of chains with hydrophobic patches.

In summary, our results demonstrate how poorly we understand protein−ligand interactions, even in relatively simple systems with extensive biophysical characterization. More, and extensive, calorimetric investigations of well-characterized protein−ligand pairs will, we believe, be required to elucidate the origin of enthalpy/entropy compensation and further our ability to exploit this phenomenon in the rational design of high-affinity ligands.

Experimental Section

General Methods. Chemicals were purchased from Aldrich, Fluka, TCI, and Bachem. Bovine carbonic anhydrase II (pI 5.9) was obtained from Sigma. *N*-Hydroxybenzotriazole (HOBt) and (benzotriazol-1-yloxy)tris(dimethylamino)phosphonium hexafluorophosphate (BOP) were purchased from Advanced Chemtech (Louisville, KY). NMR experiments were carried out on a Varian Inova 500 MHz. Isothermal titration calorimetry was performed using a VP-ITC microcalorimeter (MicroCal). Analytical HPLC was run on a Varian instrument with a C18 column, 5 μm (4.6 × 250 mm), from Vydac using a linear gradient of water with 0.1% TFA (A) followed by acetonitrile containing 0.08% TFA (B), at a flow rate of 1.2 mL min^{-1} (UV detection at 214 and 254 nm). Preparative reverse-phase HPLC was performed using a Varian Prostar HPLC system equipped with a C18 column, 5 μm (10 × 250 mm), from Vydac at a flow rate of 6 mL min^{-1} with UV detection at 214 nm.

General Procedures. *p*-$H_2NSO_2C_6H_4CO(NHCH_2CO)_nOH$ ($ArGly_nO^-$), *p*-$H_2NSO_2C_6H_4CONH(CH_2CH_2O)_nCH_3$ ($ArEG_nOMe$), and *p*-$H_2NSO_2C_6H_4CON(CH_3)CH_2COOtBu$ were prepared according to the general procedure of Jain et al.[13]

General Procedure for the Syntheses of *p*-$H_2NSO_2C_6H_4CO(N(CH_3)CH_2CO)_nOH$ ($ArSar_nO^-$) (n = 2, 3, 4, and 5). Peptide Synthesis and Characterization. The $ArSar_nO^-$ peptides were synthesized by Fmoc chemistry by the stepwise solid-phase methodology. Assembly of the protected peptide chains was carried out on a 50 μmol scale starting from a Fmoc-Sar-Trityl resin. The Fmoc group was removed using 25% piperidine in DMF (1 × 5 min, 1 × 15 min) with agitation by nitrogen. The resin was then filtered and washed with DMF (6 × 3 min). For each coupling step, a solution of the Fmoc−amino acid (5 equiv), BOP (5 equiv), and HOBt (5 equiv) in DMF and DIEA were added successively to the resin, and the suspension was mixed for 10 min. A double coupling was performed sequentially. Monitoring of the coupling reaction was performed with the chloranil test. After removal of the last group, the resin was washed with DMF and reacted with 4-carboxybenzenesulfonamide (5 equiv) with BOP (5 equiv), HOBt (5 equiv), and DIEA (5 equiv) in DMF for 1 h. The resin was washed with CH_2Cl_2 and Et_2O and dried under nitrogen. Cleavage of the peptide from the resin was performed by treatment with a mixture of trifluoroacetic acid, water, and dithiothreitol (90%:5%:5%). After precipitation in cold ether and centrifugation, the peptide was solubilized in water and lyophilized. The crude peptide derivative was purified by HPLC (linear gradient, 0−70% *B*, 40 min) and lyophilized.

^{1}H NMR of *p*-$H_2NSO_2C_6H_4CON(CH_3)CH_2COOtBu$ and *p*-$H_2NSO_2C_6H_4CO(N(CH_3)CH_2CO)_nOH$ ($ArSar_nO^-$). Because of the presence of cis (and trans) isomers for these sarcosine-containing compounds,[54] resonances become challenging to assign when there is more than one Sar residue in the chain. For all of the ligands in this series, we have assigned the resonances in the aromatic region to protons of the cis and trans isomers for the Sar residue nearest to the phenyl ring. For $ArSar_1O^-$, we have assigned the resonances for the aliphatic (methylene and *N*-methyl) protons to these conformations. For ligands with more than one Sar residue in the chain, we have reported the aliphatic resonances as ranges corresponding to the protons of all of the residues (and conformations) of the chain.

***p*-$H_2NSO_2C_6H_4CON(CH_3)CH_2COOtBu$.** HPLC t_R 13.05 min (linear gradient, 0−100% *B*, 20 min); ^{1}H NMR (500 MHz, DMSO-d_6) δ 7.91 (d, J = 8.3 Hz, 2H trans), 7.86 (d, J = 7.8 Hz, 2H cis), 7.60 (d, J = 8.3 Hz, 2H trans), 7.48 (m, 2H cis, 2H sulfonamide), 4.15 (s, 2H trans), 3.92 (s, 2H cis), 3.00 (s, 3H cis), 2.92 (s, 3H trans), 1.46 (s, 9H trans), 1.38 (s, 9H cis); HRMS *m*/*z* found 329.1174 (M + H)$^+$, calcd 329.1171.

***p*-$H_2NSO_2C_6H_4CON(CH_3)CH_2COOH$ ($ArSar_1O^-$).** *p*-$H_2NSO_2C_6H_4CON(CH_3)CH_2COOtBu$ (100 mg, 304 μmol) was dissolved in 5 mL of trifluoroacetic acid and stirred for 30 min at room temperature. The solution was evaporated to dryness. Recrystallization from 3 mL of deionized hot water yielded a crude white powder (42 mg, 154 μmol, 51%). HPLC t_R 8.61 min (linear gradient, 0−100% *B*, 20 min); ^{1}H NMR (500 MHz, DMSO-d_6) δ 7.88 (d, J = 8.3 Hz, 2H trans), 7.84 (d, J = 8.3 Hz, 2H cis), 7.58 (d, J = 8.3 Hz, 2H trans), 7.46 (m, 2H cis, 2H sulfonamide), 4.15 (s, 2H trans), 3.92 (s, 2H cis), 2.98 (s, 3H cis), 2.91 (s, 3H trans); HRMS *m*/*z* found 273.0542 (M + H)$^+$, calcd 273.0545.

***p*-$H_2NSO_2C_6H_4CO(N(CH_3)CH_2CO)_2OH$ ($ArSar_2O^-$).** HPLC t_R 8.69 min (linear gradient, 0−100% *B*, 20 min); ^{1}H NMR (500 MHz, DMSO-d_6) δ 7.88 (d, J = 8.3 Hz, 2H trans), 7.80 (m, 2H cis), 7.57 (d, J = 8.3, 2H trans), 7.46 (m, 2H cis, 2H sulfonamide), 4.39−3.98 (4H, 4.39 (s), 4.25 (s), 4.18 (s), 4.15 (s), 4.02 (s), 3.98 (m)), 3.04−2.80 (6H, 3.04 (s), 2.94 (s), 2.85 (m), 2.80 (m)); HRMS *m*/*z* found 344.0914 (M + H)$^+$, calcd 344.0916.

***p*-$H_2NSO_2C_6H_4CO(N(CH_3)CH_2CO)_3OH$ ($ArSar_3O^-$).** HPLC t_R 8.77 min (linear gradient, 0−100% *B*, 20 min); ^{1}H NMR (500 MHz, DMSO-d_6) δ 7.88 (d, J = 7.8 Hz, 2H trans), 7.81 (m, 2H cis), 7.57 (m, 2H trans), 7.45 (m, 2H cis, 2H sulfonamide), 4.39−3.95 (6H, 4.39 (m), 4.24 (m), 4.13 (m), 4.01 (m), 3.97 (m), 3.95 (s)), 3.02−2.72 (9H, 3.02−2.91 (m), 2.86−2.72 (m)); HRMS *m*/*z* found 415.1289 (M + H)$^+$, calcd 415.1287.

***p*-$H_2NSO_2C_6H_4CO(N(CH_3)CH_2CO)_4OH$ ($ArSar_4O^-$).** HPLC t_R 8.94 min (linear gradient, 0−100% *B*, 20 min); ^{1}H NMR (500 MHz, DMSO-d_6) δ 7.88 (d, J = 7.8 Hz, 2H trans), 7.80 (m, 2H cis), 7.57 (d,

(54) Evans, C. A.; Rabenste, D. L. *J. Am. Chem. Soc.* **1974**, *96*, 7312−7317.

J = 6.8, 2H trans), 7.45 (m, 2H cis, 2H sulfonamide), 4.40−3.83 (m, 8H), 3.03−2.69 (m, 12H); HRMS m/z found 486.1658 $(M + H)^+$, calcd 486.1658.

***p*-$H_2NSO_2C_6H_4CO(N(CH_3)CH_2CO)_5OH$ ($ArSar_5O^-$).** HPLC t_R 9.06 min (linear gradient, 0−100% *B*, 20 min); ^{1}H NMR (500 MHz, DMSO-d_6) δ 7.88 (d, J = 7.8 Hz, 2H trans), 7.80 (m, 2H cis), 7.57 (d, J = 8.3 Hz, 2H trans), 7.45 (m, 2H cis, 2H sulfonamide), 4.38−3.81 (m, 10H), 3.03−2.70 (m, 15H); HRMS m/z found 557.2031 $(M + H)^+$, calcd 557.2029.

NMR Quantitation of Stock Solutions of Arylsulfonamide Ligands. Arylsulfonamide ligands were prepared gravimetrically to ~20 mM in DMSO-d_6. Stock solutions were diluted 1:10 with 2.00 mM maleic acid in DMSO-d_6, prepared gravimetrically. Proton resonances from the arylsulfonamide were normalized relative to those from of maleic acid (allowing a 10 s delay between pulses) to determine accurately the concentration of the stock solutions.

Isothermal Titration Calorimetry. To determine values of $\Delta H°$ and K_d, ~10 μM BCA II (concentration determined by UV spectrophotometry, ϵ_{280} = 57 000 M^{-1} cm^{-1})[33] in 20 mM sodium phosphate buffer pH 7.5 (with 0.6% DMSO-d_6) was titrated with ~110 μM arylsulfonamide ligand (concentration determined by ^{1}H NMR) in the same buffer at T = 298 K. Twenty-five 12.0 μL injections were preceded by one 2.0 μL injection, which was omitted for data analysis. After subtraction of background heats, the data were analyzed by a single-site binding model using the Origin software (provided by Microcal) with the values of binding stoichiometry, $\Delta H°$, and K_d being allowed to vary to optimize the fit. Measurements were conducted 2−4 times. For measurements of ΔC_p, solutions of arylsulfonamide >1 mM (>1000K_d) in 20 mM sodium phosphate pH 7.5 were titrated with at least seven 10 μL injections of ~100 μM BCA (concentration determined by UV spectrophotometry) in the same buffer. The individual peaks were averaged, subtracted by the heat of dilution of protein into buffer alone (without ligand), and normalized to the number of moles of BCA added to yield an estimate of $\Delta H°$. These measurements were conducted at 288, 298, and 308 K. Linear-regression analysis of $\Delta H°$ vs T gave an estimate of ΔC_p.

Acknowledgment. This work was supported by the National Institutes of Health (GM51559 and GM30367). V.M.K. and B.R.B. acknowledge support from pre-doctoral fellowships from the NDSEG and NSF, respectively. V.S. acknowledges support from La Ligue Contre Le Cancer (France).

JA060070R